Mini-magnetosphere over the Reiner Gamma magnetic anomaly region on the Moon

M. Kurata,[1] H. Tsunakawa,[1] Y. Saito,[2] H. Shibuya,[3] M. Matsushima,[1] and H. Shimizu[4]

Received 16 July 2005; revised 31 August 2005; accepted 14 September 2005; published 28 December 2005.

[1] We show presence of a mini-magnetosphere above the Reiner Gamma magnetic anomaly (RGA) region in the solar wind, using Lunar Prospector magnetometer (MAG) measurement data. RGA is one of the strongest magnetic anomalies on the Moon. Two magnetic anomalies are found from six MAG datasets at 17–40 km altitudes in the lunar wake or the geomagnetic tail lobe and are well explained by a two-dipole model. When RGA was exposed to the solar wind plasma, two MAG datasets were obtained at 27–29 km altitudes. Although the magnetic anomalies survived against the plasma pressure, they were heavily distorted in comparison with the magnetic field of the two-dipole model. Flow directions and dynamic pressures of the solar wind plasma at those periods indicate that the distortions were caused by forming a mini-magnetosphere over the RGA region in the solar wind. **Citation:** Kurata, M., H. Tsunakawa, Y. Saito, H. Shibuya, M. Matsushima, and H. Shimizu (2005), Mini-magnetosphere over the Reiner Gamma magnetic anomaly region on the Moon, *Geophys. Res. Lett.*, *32*, L24205, doi:10.1029/2005GL024097.

1. Introduction

[2] Since unusual albedo markings are found around several lunar magnetic anomalies [e.g., *Hood et al.*, 1979, 2001; *Richmond et al.*, 2003], it has been proposed that relatively strong magnetic anomalies have deflected the solar wind plasma [e.g., *Dyal et al.*, 1972; *Hood*, 1980] and preserved the area against optical maturation (darkening with time) for a few billion years [e.g., *Hood and Schubert*, 1980; *Hood and Williams*, 1989; *Richmond et al.*, 2005]. It has recently been reported that anomalously strong magnetic fields were detected from a few orbital observations by magnetometer (MAG) of Lunar Prospector (LP) in the solar wind downstream of the magnetic anomaly in Imbrium antipode region, which was interpreted as presence of a mini-magnetosphere [*Lin et al.*, 1998]. Also MHD (magnetohydrodynamic) and particle simulations have demonstrated a mini-magnetosphere over a lunar magnetic anomaly [*Harnett and Winglee*, 2000, 2002, 2003], stressing that the mini-magnetosphere structure is interesting for plasma physics since its size is comparable to the scale of the transition between particle and fluid behaviors. From practical aspects, the anomaly region would give a feasible place for the future lunar base if the mini-magnetosphere works as a shelter against the solar wind plasma. It is thus very important to clearly reveal whether a mini-magnetosphere exists above a lunar magnetic anomaly in the solar wind. In this study, we have explored LP MAG low-altitude (17–40 km) data for a mini-magnetosphere above Reiner Gamma magnetic anomaly (RGA) region in the western part of Oceanus Procellarium (~58 W, ~8 N), which is one of the strongest magnetic anomalies accompanied with unusual albedo markings [*Hood et al.*, 1979; *Hood and Schubert*, 1980; *Hood et al.*, 2001; *Pinet et al.*, 2000].

2. Two-Dipole Model of RGA Fields

[3] We used level-1 MAG data of the time series at 5 second intervals taken from NASA Planetary Data System node at University of California, Los Angeles, and analyzed the magnetic field data. After transforming the data into the lunar radial, east, and north coordinates along each orbit and removing the temporal low-frequency variation mainly due to the interplanetary magnetic field (IMF) changes [*Hood et al.*, 1981], residual magnetic fields were represented as magnetic anomaly fields. Although the electron reflection (ER) data are also available, we have concentrated on the MAG data for the present analysis.

[4] First we analyzed RGA magnetic field data in the lunar wake or the geomagnetic tail lobe, where densities of the solar wind plasma are so low that magnetic anomaly fields are almost undisturbed [*Hood et al.*, 1981, 2001]. Data segments with good quality [*Hood et al.*, 2001] were selected from 6 periods: 1 period in the tail lobe and 5 periods in the lunar wake (Table 1). Selenographical distribution of all the data points (N = 1509) ranges in 53–62 W in longitudes, 4–13 N in latitudes and 17–40 km in altitudes. Two magnetic anomalies of the southwest part (SW) and the northeast part (NE) are detected for each period as reported by *Hood et al.* [2001]. Examples of the contour map of the observed magnetic field are shown for days 81–82 (18–19 km altitudes) in Figure 1, where maximum total intensity is about 50 nT at the center of SW anomaly.

[5] We modeled SW and NE anomalies in terms of two magnetic dipoles. Optimal values of those positions and three components of magnetic dipole moments were determined by iterative procedures [*Von Frese et al.*, 1981; *Dyment and Arkani-Hamned*, 1998]. We confirmed robustness of the solutions trying several different initial values. The optimal solutions of a dipole position (longitude, latitude and depth), a dipole direction (inclination I and declination D) and a dipole moment are (58.4W, 7.5N, 11.1 km, 1.3 deg, −11.0 deg, 11.3×10^{12} Am^2) for SW and (55.3W, 10.9N, 6.7 km, 3.7 deg, −68.7 deg, 3.5×10^{12} Am^2) for NE, where the inclination I is the angle from

[1]Department of Earth and Planetary Sciences, Tokyo Institute of Technology, Tokyo, Japan.
[2]Institute of Space and Astronautical Science, Japan Aerospace Exploration Agency, Kanagawa, Japan.
[3]Department of Earth Sciences, Kumamoto University, Kumamoto, Japan.
[4]Earthquake Research Institute, University of Tokyo, Tokyo, Japan.

0094-8276/05/2005GL024097

Table 1. Observational Periods of the Reiner Gamma Magnetic Anomaly (RGA) Region Analyzed in the Present Study[a]

			Solar Wind Plasma Flow			
Day(s) of 1999	Condition	Altitude, km	θ, deg	φ, deg	P_{sw}, nPa	Remark
54	lunar wake	7.6–19.2	—	—	—	
81–82	lunar wake	17.1–18.8	—	—	—	Figure 1
109	lunar wake	17.1–18.3	—	—	—	
136	lunar wake	33.0–35.1	—	—	—	
149–150	tail lobe	37.5–39.7	—	—	—	
163–164	lunar wake	32.7–34.8	—	—	—	
40–41	solar wind	26.0–28.2	37–38	79–86	<1	Figure 2
68	solar wind	27.5–28.7	62–66	61–78	2.5–4.5	Figure 3

[a]Day: observational day of 1999 (e.g., 1 = February 1st of 1999), θ: the dip angle of the solar wind plasma flow direction at RGA (e.g., θ = 0: horizontal, θ = 90: vertical and downward), φ: the azimuthal angle (e.g., φ = 0: northward, φ = 90: eastward). These angles are calculated assuming that the solar wind plasma flows radially from the sun. P_{sw}: dynamic pressure of the solar wind plasma (= ρv^2, where ρ and v are the solar wind mass density and flow velocity, respectively) derived from ACE spacecraft data time-shifted to LP's position to allow for the solar wind travel time from ACE to LP [*Lin et al.*, 1998].

the horizontal plane (downward direction is positive) and the declination D is the angle from the north (clockwise rotation is positive). The resultant direction of the SW dipole is not far from those given by the several-disk model applied to the Apollo data (only for SW anomaly; I = −39 to −50 deg, D = −24 to −36 deg) in previous study [*Hood*, 1980].

[6] Model fields of the two dipole sources were calculated for the same observational positions as those of the observational days and compared with the observed magnetic fields. The contour configurations of the observed fields are well reproduced by the two-dipole model with a root mean square value of 1.8 nT in total intensities for all the data points. Examples of relatively low altitudes are shown for days 81–82 as contour maps of A-mod in Figure 1. Compared with the high altitude datasets, magnetic fields of the two-dipole model also show good coincidence with the observations. Thus a magnetic field at an arbitrary position above the RGA region can be estimated from the two-dipole model if the magnetic field is undisturbed by the solar wind plasma.

3. RGA Fields in the Solar Wind

[7] The magnetic fields of RGA exposed to the solar wind plasma, that is in the day side, are shown in Figure 2 for days 40–41 and in Figure 3 for day 68. Dynamic pressure (P_{sw}) and flow direction angles (θ and φ) of the solar wind in the RGA region are listed for these periods in Table 1, where θ and φ are the angle from the horizontal plane (downward direction is positive) and the angle from the north (clockwise rotation is positive), respectively. These directions were estimated from the ACE (Advanced Composition Explorer) spacecraft data time-shifted to LP's positions [*Lin et al.*, 1998] since ACE is located at Earth-Sun Lagrange point (L1).

[8] Contour configurations in Figures 2 and 3, particularly near SW anomaly, indicate that the magnetic anomalies survived above the RGA region even in the solar wind. The two-dipole model fields are shown as B-mod (Figure 2) and C-mod (Figure 3) assuming the same observational positions of LP as those for days 40–41 (B) and day 68 (C), respectively. Since both the observational altitudes range in 26–29 km, the model field calculation is almost equivalent to interpolation using the six datasets of RGA in the lunar wake or the tail lobe (17–40 km altitudes).

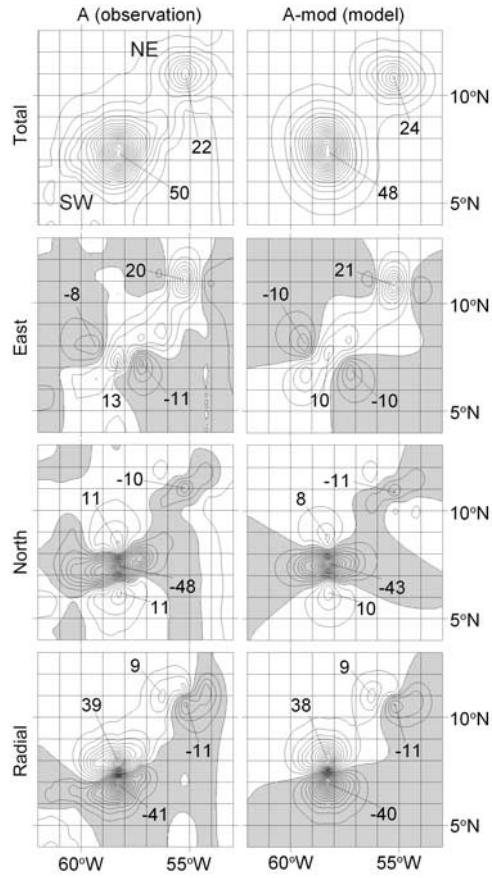

Figure 1. Representative examples of contour maps of the magnetic fields for total intensity and three components (north, east and radial) from Lunar Prospector (LP) observations above the Reiner Gamma magnetic anomaly (RGA) region in the western part of Oceanus Procellarium under almost no influences of the solar wind plasma. A: the observed magnetic field for days 81–82 at altitudes of 17.1–18.8 km when the RGA region was in the lunar wake. A-mod: model fields calculated from the two-dipole model at the same observational positions as those of A (see the text). Contour intervals are 2.5 nT and negative magnetic fields are shaded. The spatial resolution is estimated to be about ±0.5 deg (±15 km) in longitudes and ±0.13 deg (±4 km) in latitudes considering the distribution of the observational points.

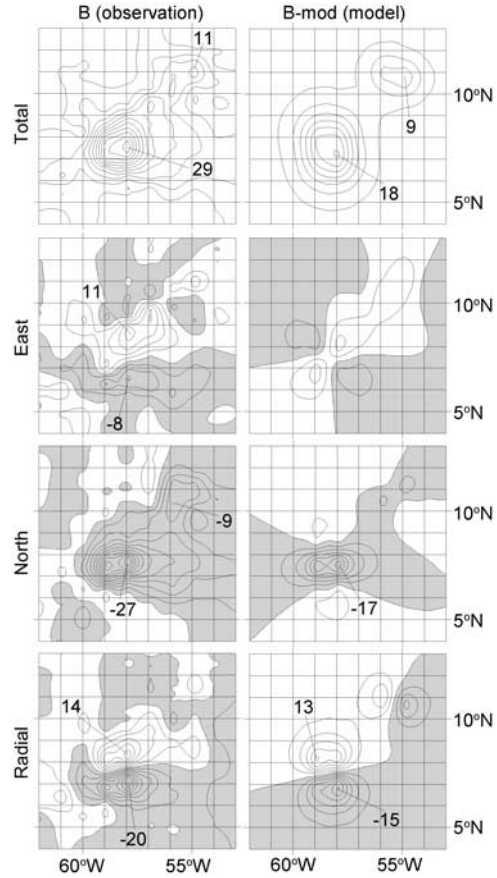

Figure 2. Magnetic fields observed for days 40–41 at altitudes of 26.0–28.4 km (B) when the RGA region was exposed to the solar wind plasma, and model fields (B-mod) calculated from the two-dipole model at the same positions as those of B. The solar wind plasma at that period flowed nearly eastward with a relatively shallow dip angle and a low dynamic pressure (see Table 1).

[9] It is clearly seen in Figures 2 and 3 that contour configurations of the observed magnetic field in the solar wind are heavily distorted in comparison with those of the two-dipole model. Major distortions of the observed magnetic field from B-mod (Figure 2) are that (1) maximum total intensity in the observation (29 nT) is stronger than in the model (18 nT) and (2) contour patterns of the east component and total intensity in the observation are elongated eastward, that is, towards the downstream of the solar wind plasma flow (see Table 1). Major distortions of the observed magnetic field from C-mod (Figure 3) are that (1) maximum total intensity in the observation (35 nT) is much stronger than in the model (19 nT), (2) horizontal size of the anomaly in the observation is reduced to about a half of that in the model, and (3) a ratio of the maximum radial component to the maximum total intensity in the observation (13 nT/35 nT = 0.37) is much smaller than in the model (16 nT/19 nT = 0.84).

4. Discussion

[10] We examine the characteristic distortions of the magnetic field above RGA considering interaction with the solar wind plasma. For simplicity, SW anomaly is represented by a single dipole source of a horizontal and northward magnetic moment (I = D = 0) while NE anomaly is ignored. Here three conditions of the solar wind plasma flow are assumed: (I) no solar wind, (II) $\theta = 0$ deg and $\varphi = 90$ deg (horizontal and eastward flow), and (III) $\theta = 90$ deg (vertical and downward flow). In case I, which corresponds to the lunar wake or the geomagnetic tail lobe (Figure 1), the contour pattern should be symmetric or antisymmetric with respect to the meridian line because of I = D = 0. In case II, the solar wind plasma would exert a force as if magnetic lines of force are pulled eastward resulting in asymmetric contour patterns of magnetic fields about the meridian line. If there is a mini-magnetosphere, magnetic lines of force would concentrate near its magnetopause and thus total intensity would be stronger there than at the same altitudes of case I. In case III, the solar wind plasma would exert a force as if magnetic lines of force are compressed downward and thus the magnetic anomaly would be confined to a narrower region than in case I. Maximum total intensity of the anomaly field in case III would be largest and the field direction would be more horizontal near the top of magnetopause.

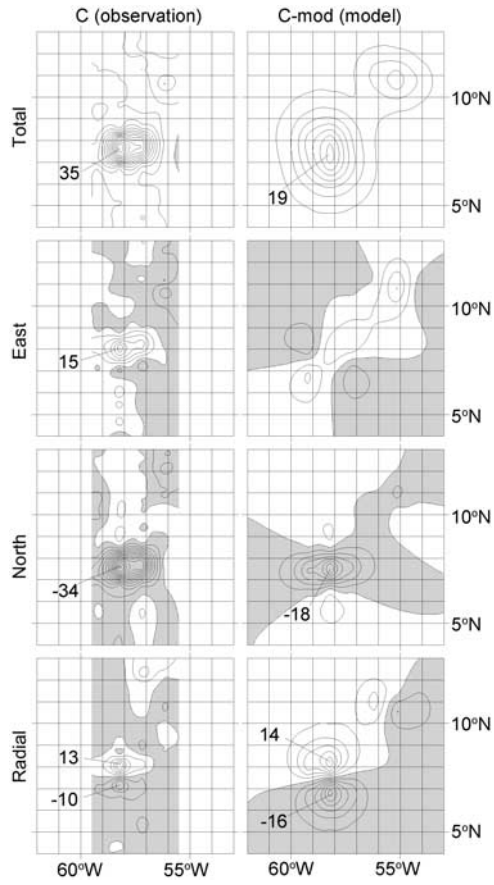

Figure 3. Magnetic fields observed for day 68 at altitudes of 26.7–29.1 km (C) when RGA was exposed to the solar wind plasma, and model fields (C-mod) calculated from the two-dipole model at the same positions as those of C. The solar wind plasma at that period flowed with a deep dip angle and a high dynamic pressure (see Table 1).

[11] The plasma flow direction for days 40–41 was almost eastward and moderately horizontal (θ = 37–38 deg) like case II, while that for day 68 was relatively vertical-downward (θ = 62–66 deg) like case III. It should be noted that the major distortions of days 40–41 and day 68 are similar to those of case II and case III, respectively. Besides, P_{sw} of day 68 is estimated to have been a few times higher than that of days 40–41, thus magnetic lines of force could be compressed more efficiently and also the field intensity could be stronger as seen in Figure 3. This suggests that LP was traveling slightly below the magnetopause for days 40–41 and day 68 and the vertical size of RGA mini-magnetosphere is estimated from LP's altitudes to have been about 30 km or more.

[12] It is noteworthy that the size of the compressed magnetic anomaly in Figure 3 is comparable to that of the observed albedo marking in the RGA region. This may support that albedo marking is resulted from prevention against the solar wind plasma alteration by the mini-magnetosphere [e.g., *Hood and Schubert*, 1980]. The effect of dipole deflections and intensities would be evaluated by the computer simulation.

5. Conclusions

[13] The magnetic anomalies survived above the RGA region in the solar wind and showed particular distortions due to the interaction with the solar wind plasma. This strongly suggests that a mini-magnetosphere was presented over the RGA region in the solar wind and its vertical size is estimated to have been about 30 km or more. The detailed structure of RGA mini-magnetosphere would be clarified by magnetic-field and plasma-particle observations at altitudes of about 30 km or less in the future mission.

[14] **Acknowledgments.** Lunar Prospector MAG dataset (level-1) used in this study was provided through NASA PDS node at University of California, Los Angeles. We thank T. Nagai for processing the IMF data and J. Haruyama for helpful discussions. We also thank two anonymous reviewers for valuable comments.

References

Dyal, P., C. W. Parkin, C. W. Snyder, and D. R. Clay (1972), Measurements of lunar magnetic field interaction with the solar wind, *Nature*, *236*, 381–385.

Dyment, J., and J. Arkani-Hamned (1998), Equivalent source magnetic dipoles revisited, *Geophys. Res. Lett.*, *25*, 2003–2006.

Harnett, E., and R. M. Winglee (2000), Two-dimensional MHD simulation of the solar wind interaction with magnetic field anomalies on the surface of the Moon, *J. Geophys. Res.*, *105*, 24,997–25,007.

Harnett, E. M., and R. M. Winglee (2002), 2.5D Particle and MHD simulations of mini-magnetospheres at the Moon, *J. Geophys. Res.*, *107*(A12), 1421, doi:10.1029/2002JA009241.

Harnett, E. M., and R. M. Winglee (2003), 2.5-D fluid simulations of the solar wind interacting with multiple dipoles on the surface of the Moon, *J. Geophys. Res.*, *108*(A2), 1088, doi:10.1029/2002JA009617.

Hood, L. L. (1980), Bulk magnetization properties of the Fra Mauro and Reiner Gamma formations, *Proc. Lunar Planet. Sci. Conf.*, *11th*, 1879–1896.

Hood, L. L., and G. Schubert (1980), Lunar magnetic anomalies and surface optical properties, *Science*, *208*, 49–51.

Hood, L. L., and C. Williams (1989), The lunar swirls: Distribution and possible origins, *Proc. Lunar Planet. Sci. Conf.*, *19th*, 99–113.

Hood, L. L., P. J. Coleman Jr., and D. E. Wilhelms (1979), Lunar nearside magnetic anomalies, *Proc. Lunar Planet. Sci. Conf.*, *10th*, 2235–2257.

Hood, L. L., C. T. Russell, and P. J. Coleman Jr. (1981), Contour maps of lunar remanent magnetic fields, *J. Geophys. Res.*, *86*, 1055–1069.

Hood, L. L., A. Zakharian, J. S. Halekas, D. L. Mitchell, R. P. Lin, M. H. Acuña, and A. B. Binder (2001), Initial mapping and interpretation of lunar crustal magnetic anomalies using Lunar Prospector magnetometer data, *J. Geophys. Res.*, *106*, 27,825–27,839.

Lin, R. P., D. L. Mitchell, D. W. Curtis, K. A. Anderson, C. W. Carlson, J. McFadden, M. H. Acuña, L. L. Hood, and A. B. Binder (1998), Lunar surface magnetic fields and their interaction with the solar wind: Results from Lunar Prospector, *Science*, *281*, 1480–1484.

Pinet, P. C., V. V. Shevchenko, S. D. Chevrel, Y. Daydou, and C. Rosemberg (2000), Local and regional lunar regolith characteristics at Reiner Gamma Formation: Optical and spectroscopic properties from Clementine and Earth-based data, *J. Geophys. Res.*, *105*, 9457–9475.

Richmond, N. C., L. L. Hood, J. S. Halekas, D. L. Mitchell, R. P. Lin, M. H. Acuña, and A. B. Binder (2003), Correlation of a strong lunar magnetic anomaly with a high-albedo region of the Descartes mountains, *Geophys. Res. Lett.*, *30*(7), 1395, doi:10.1029/2003GL016938.

Richmond, N. C., L. L. Hood, D. L. Mitchell, R. P. Lin, M. H. Acuña, and A. B. Binder (2005), Correlations between magnetic anomalies and surface geology antipodal to lunar impact basins, *J. Geophys. Res.*, *110*, E05011, doi:10.1029/2005JE002405.

Von Frese, R. R. B., W. J. Hintze, and L. W. Braile (1981), Spherical Earth gravity and magnetic anomaly analysis by equivalent point source inversion, *Earth Planet. Sci. Lett.*, *53*, 69–83.

M. Kurata, M. Matsushima, and H. Tsunakawa, Department of Earth and Planetary Sciences, Tokyo Institute of Technology, 2-12-1 Okayama, Meguro, Tokyo 152-8551, Japan. (htsuna@geo.titech.ac.jp)

Y. Saito, Institute of Space and Astronautical Science, Japan Aerospace Exploration Agency, 3-1-1 Yoshinodai, Sagamihara, Kanagawa 229-8510, Japan.

H. Shibuya, Department of Earth Sciences, Kumamoto University, Kurokami 2-39-1, Kumamoto 860-8555, Japan.

H. Shimizu, Earthquake Research Institute, University of Tokyo, 1-1-1 Yayoi, Bunkyo-ku, Tokyo 113-0032, Japan.